

## RESEARCH ARTICLE

10.1002/2016JB013595

## Key Points:

- The enclosed location and large magnitudes of the Caspian Sea level change provide a unique base for validating GRACE measurements
- After appropriate leakage corrections, estimates from both GRACE spherical harmonics and mascons agree well with altimeter observations
- The forward modeled GRACE spherical harmonic estimates are in complete agreement with altimeter observations at broad time scales

## Correspondence to:

J. L. Chen,  
chen@csr.utexas.edu

## Citation:

Chen, J. L., C. R. Wilson, B. D. Tapley, H. Save, and J.-F. Cretaux (2017), Long-term and seasonal Caspian Sea level change from satellite gravity and altimeter measurements, *J. Geophys. Res. Solid Earth*, 122, 2274–2290, doi:10.1002/2016JB013595.

Received 27 SEP 2016

Accepted 17 FEB 2017

Accepted article online 20 FEB 2017

Published online 6 MAR 2017

## Long-term and seasonal Caspian Sea level change from satellite gravity and altimeter measurements

J. L. Chen<sup>1</sup> , C. R. Wilson<sup>1,2</sup> , B. D. Tapley<sup>1</sup> , H. Save<sup>1</sup> , and Jean-Francois Cretaux<sup>3</sup>

<sup>1</sup>Center for Space Research, University of Texas at Austin, Austin, Texas, USA, <sup>2</sup>Department of Geological Sciences, Jackson School of Geosciences, University of Texas at Austin, Austin, Texas, USA, <sup>3</sup>Legos/CNES, Toulouse, France

**Abstract** We examine recent Caspian Sea level change by using both satellite radar altimetry and satellite gravity data. The altimetry record for 2002–2015 shows a declining level at a rate that is approximately 20 times greater than the rate of global sea level rise. Seasonal fluctuations are also much larger than in the world oceans. With a clearly defined geographic region and dominant signal magnitude, variations in the sea level and associated mass changes provide an excellent way to compare various approaches for processing satellite gravity data. An altimeter time series derived from several successive satellite missions is compared with mass measurements inferred from Gravity Recovery and Climate Experiment (GRACE) data in the form of both spherical harmonic (SH) and mass concentration (mascon) solutions. After correcting for spatial leakage in GRACE SH estimates by constrained forward modeling and accounting for steric and terrestrial water processes, GRACE and altimeter observations are in complete agreement at seasonal and longer time scales, including linear trends. This demonstrates that removal of spatial leakage error in GRACE SH estimates is both possible and critical to improving their accuracy and spatial resolution. Excellent agreement between GRACE and altimeter estimates also provides confirmation of steric Caspian Sea level change estimates. GRACE mascon estimates (both the Jet Propulsion Laboratory (JPL) coastline resolution improvement version 2 solution and the Center for Space Research (CSR) regularized) are also affected by leakage error. After leakage corrections, both JPL and CSR mascon solutions also agree well with altimeter observations. However, accurate quantification of leakage bias in GRACE mascon solutions is a more challenging problem.

### 1. Introduction

The Caspian Sea is the largest enclosed inland body of water on Earth, with a surface area of ~371,000 km<sup>2</sup>. Located within an endorheic (no outflow) basin between Europe and Asia, it is surrounded by five countries (Russia, Kazakhstan, Turkmenistan, Iran, and Azerbaijan) (Figure 1) and has a sea level history independent of global ocean eustatic changes. Average Caspian Sea level is currently about 27.5 m below mean sea level. With characteristics of both oceans and lakes, the Caspian Sea is often classified as the world's largest lake, containing about 3.5 times more water, by volume, than all five of North America's Great Lakes combined [[https://en.wikipedia.org/wiki/Caspian\\_Sea](https://en.wikipedia.org/wiki/Caspian_Sea)].

Caspian Sea level has undergone substantial fluctuations during the past several hundred years [*Klige and Myagkov*, 1992; *Panin*, 2007], including changes of several meters within a few decades in the recent past [*Cazenave et al.*, 1997; *Panin*, 2007]. These longer period and seasonal level variations are enormous when compared with global sea level seasonal changes and long-term rates of a few millimeters per year. Caspian Sea level reflects a balance between river inflow and evaporation. About 90% of the inflow comes from the north, mainly from the Volga (80%), with another ~10% from the Ural. Because fluctuations in precipitation within the Caspian drainage basin are the dominant influence on both inflow and evaporation, Caspian Sea level changes provide an important measure of global and regional climate change. The large magnitudes and spatial scales of the Caspian Sea level change also offer a unique opportunity for validating different time-variable gravity solutions and mass change products from the Gravity Recovery and Climate Change (GRACE) mission [*Tapley et al.*, 2004].

Satellite radar altimeter observations of global sea surface height (SSH) change are available since 1992, when the TOPEX/Poseidon radar altimeter mission was launched [*Fu and Davidson*, 1995; *Alsdorf et al.*, 2001]. Combined observations from TOPEX/Poseidon and a series of follow-on missions (Jason-1, Jason-2, and Jason-3) provide over two decades of continuous measurements of SSH, enabling studies of both global and regional sea level change. Figure 2 shows monthly Caspian Sea level change for the period of October 1992



**Figure 1.** Map of the Caspian Sea and surrounding countries (modified from an original map provided by the Nations Online Project at <http://www.nationsonline.org/>).

to April 2015, from the multisatellite SSH solution of Legos/Centre National d'Etudes Spatiales (CNES) [Cretaux *et al.*, 2011, 2016]. Figure 2 shows a decreasing trend and superimposed large seasonal oscillations with peak-to-peak variations up to 40 cm. In comparison, seasonal variations in the oceans at the same latitude are around 10 cm [Chen *et al.*, 2000]. Figure 2 shows that, over the past decade (April 2005 to April 2015), Caspian Sea level has been dropping at an average rate of  $\sim -9.0 \pm 0.2$  cm/yr, while over the same period, global mean sea level has risen at a rate near 0.3 cm/yr [Yi *et al.*, 2015].

The Gravity Recovery and Climate Experiment (GRACE) measures time variations in Earth's gravity field and has provided an entirely new remote sensing tool to monitor large-scale mass redistribution within the Earth system [Tapley *et al.*, 2004]. Since its launch in March 2002, GRACE has revolutionized many studies related to Earth's climate, including those of terrestrial water storage (TWS) [e.g., Wahr *et al.*, 2004; Schmidt *et al.*, 2006; Rodell *et al.*, 2009], ice mass changes over polar ice sheets and mountain glaciers [Velicogna and Wahr, 2006; Chen *et al.*, 2006, 2007; Wouters *et al.*, 2008], and sea level change [e.g., Chambers *et al.*, 2004; Chen *et al.*, 2005; Cazenave and Chen, 2010; Ogawa *et al.*, 2011]. GRACE time-variable gravity measurements have also provided an important tool for studying solid Earth geophysics and geodynamics, such as glacial isostatic adjustment (GIA) [e.g., Tamisiea *et al.*, 2007] and Earth rotation [e.g., Chen *et al.*, 2013; Adhikari and Ivins, 2016]. While satellite altimetry has been successful in measuring SSH, GRACE offers a unique measure of the mass change component of SSH, leading to independent understanding of other contributors such as steric effects [e.g., Chambers, 2006].

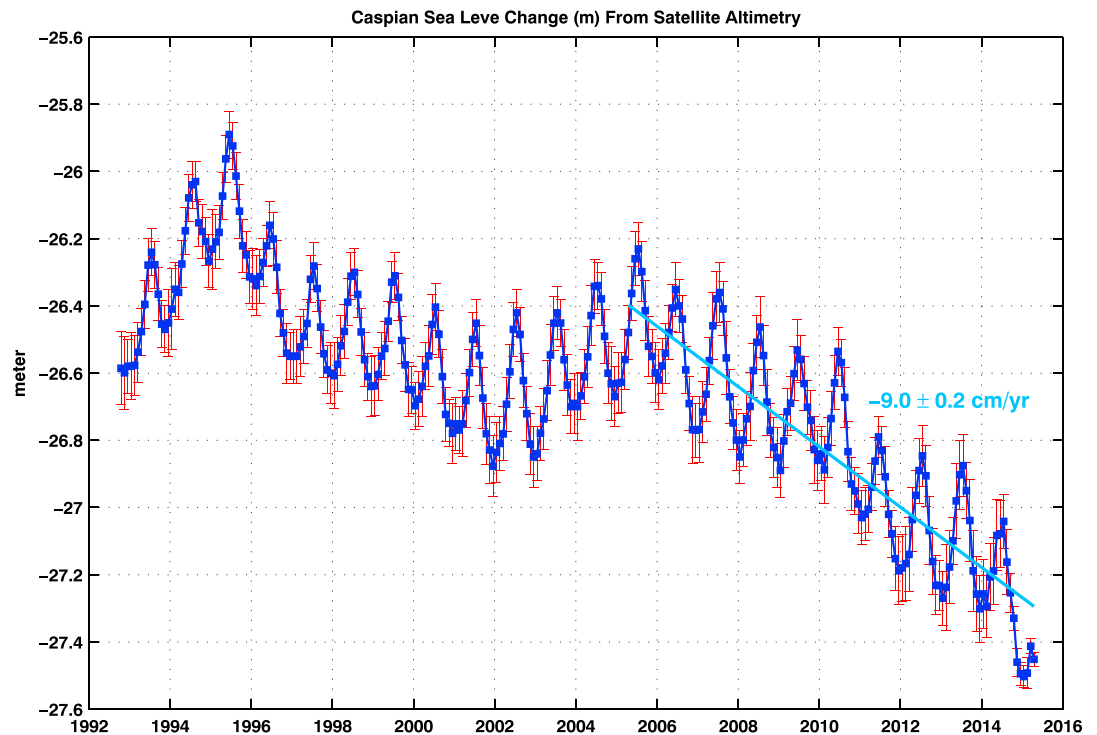


**Figure 2.** Monthly mean sea surface height (SSH) changes of the Caspian Sea observed by satellite altimetry over the period of October 1992 to April 2015 (provided by Legos/CNES, <http://hydroweb.theia-land.fr/>).

Extracting quantitative measures of surface mass changes from GRACE measurements is a challenging problem. The GRACE orbit configuration (inclination, altitude, and separation of the twin satellites) determines temporal and spatial sampling properties, making it necessary to filter solutions to suppress spatial noise in high degree and order spherical harmonics (SH) and limiting spatial resolution to 200–500 km [Chen *et al.*, 2016]. GRACE mascon (mass concentration) solutions offer improved spatial resolution (than those from SH solutions), but people still need to address the leakage appropriately in order to study regional mass change [Schrama *et al.*, 2014]. In regions containing several sources of mass change (such as TWS, mountain glaciers, and polar ice sheets), this lack of spatial resolution makes it difficult to study individual components (such as mountain glaciers) without independent measures of the other contributions [Gardner *et al.*, 2011]. In addition, there are few in situ measurements of surface mass (gravity) changes to validate GRACE estimates. Small-scale (or point-wise) in situ measurements are not easily compared with GRACE solutions [e.g., Crossley *et al.*, 2013], which represent large-scale (200–500 km) averages.

Caspian Sea seasonal level changes ( $\sim 40$  cm peak-to-peak) exceed TWS changes in most middle-to-high latitude river basins [Humphrey *et al.*, 2016]. Similarly, the linear trend over the past decade ( $\sim -9.0 \pm 0.2$  cm/yr) is greater than TWS trends in most of the world [Humphrey *et al.*, 2016]. Thus, Caspian Sea level observations from mm-precise satellite altimetry offer an important means to validate the GRACE solutions. They provide both the necessary large spatial scale and magnitude to enable separation from other signals. The purpose of this study is to compare altimeter observations with GRACE estimates derived by using different data processing methods including both SH and mascon solutions. This will improve understanding of GRACE estimates in their various forms, including validation of processing methods and identification of limitations and biases.

## 2. Data Processing

### 2.1. GRACE Spherical Harmonic Solutions

The GRACE data used here include 144 monthly Release 5 (RL05) gravity solutions from April 2002 to April 2015, provided by the Center for Space Research (CSR) at the University of Texas at Austin. Each monthly

field consists of fully normalized SH coefficients up to degree and order 60, and the degree-2 zonal harmonic coefficients are replaced by satellite laser ranging estimates provided by CSR [Cheng and Ries, 2015]. Seasonal geocenter change estimates are determined by using the method of Swenson *et al.* [2008], but no long-term geocenter estimates are available. Atmospheric, oceanic, and tidal effects have been removed during GRACE processing by using models for climate and ocean circulation effects [Bettadpur, 2012]. The Caspian Sea is not included in the ocean model. GRACE estimates of mass changes over land are dominantly a sum of TWS (groundwater, lake storage, and soil moisture) and ice mass changes (in glaciated and permafrost regions). Lake storage variations are the dominant signal in the Caspian Sea region.

The regional gravity variations from GRACE high degree and order SH coefficients are contaminated by spatial noise, which includes longitudinal stripes and other errors. The longitudinal stripes are associated with correlations between even and odd degree SH coefficient pairs of a given order [Swenson and Wahr, 2006]. Therefore, a decorrelation filter is commonly used to suppress the stripe noise, and Gaussian smoothing is also applied to further reduce residual high SH degree error. While the decorrelation filter suppresses longitudinal stripe noise, it also attenuates mass change signals, especially where longitudinal (north-south) mass change patterns are present [Swenson and Wahr, 2006; Chen *et al.*, 2011]. Given that the Caspian Sea has a north-south orientation, we examine SH solutions both with and without decorrelation filtering. A 300 km Gaussian smoothing is applied in both cases. Solid Earth deformation effects due to GIA are removed by using a numerical global GIA model [A *et al.*, 2013]. However, GIA effects in the Caspian Sea region are small. It is worth noting that the Caspian Sea level had dropped about 3 m over the century between 1875 and 1975 [Cazenave *et al.*, 1997], and this appears to be in a range (spatially and temporally) that might generate some anelastic, or possibly viscous, uplift response. Quantification of this potential response is beyond the scope of the present study.

After these processing steps, globally gridded  $1^\circ \times 1^\circ$  fields of surface mass change in units of equivalent water height (EWH) are calculated from every monthly GRACE SH solution, following the equations of Wahr *et al.* [1998], up to SH degree and order 60. GRACE Caspian Sea level change time series (units of EWH in cm) are then extracted from monthly mass fields by using a  $1^\circ \times 1^\circ$  basin mask for the Caspian Sea. The basin mask total area of  $\sim 368,101 \text{ km}^2$  is within 0.8% of the published value ( $371,000 \text{ km}^2$ ).

## 2.2. Leakage Error Correction of GRACE Estimates

GRACE mass change estimates from SH solutions are subject to large spatial leakage error associated with the limited SH range (degree and order 60 in the present analysis) and additional Gaussian smoothing [Chen *et al.*, 2014]. Leakage can produce significant attenuation of mass change signals when mass changes in surrounding regions are relatively small [Chen *et al.*, 2015]. Forward modeling has been proven useful for correcting or reducing leakage bias, especially when source locations of mass change signals are known [e.g., Chen *et al.*, 2006, 2007; Wouters *et al.*, 2008; Ivins *et al.*, 2011]. In a case study using synthetic data, Chen *et al.* [2015] demonstrated that, in Antarctica, where leakage attenuation can reach over 50%, knowledge of mass change in both time and space allows for the construction of a forward model to almost completely remove the bias.

The known geography of the Caspian Sea allows us to use constrained forward modeling to determine leakage biases in GRACE linear mass rates fit to time series at each grid point. Mass rates determined from several years of data are averages over time that should be less contaminated by noise than individual time series samples [Chen *et al.*, 2015]. Leakage biases for mass rates should be similar to biases at other time scales. Figure 3a shows GRACE mass rates over the Caspian Sea and surrounding regions determined from SH time series for the period of April 2002 to April 2015; 300 km Gaussian smoothing was applied, but no decorrelation filter. Spatial leakage of the signal into regions outside the Caspian Sea is obvious. The average apparent mass rate over the Caspian Sea mask is  $-2.40 \text{ cm/yr}$  (equivalent to  $-8.85 \text{ Gt/yr}$ ).

Forward modeling is an iterative process that finds a mass change (or mass change rate) that agrees with GRACE data but is confined to regions constrained by known geography. Forward modelling accounts for all processing steps such as Gaussian smoothing (Figure 3b), and differences between forward model solutions and GRACE observations are very small (Figure 3c). We assume that all mass rate variations are located within the Caspian Sea and that mass rates for TWS in surrounding regions are approximately zero. Effects of TWS contamination are examined below. After 30 iterations of constrained forward modeling

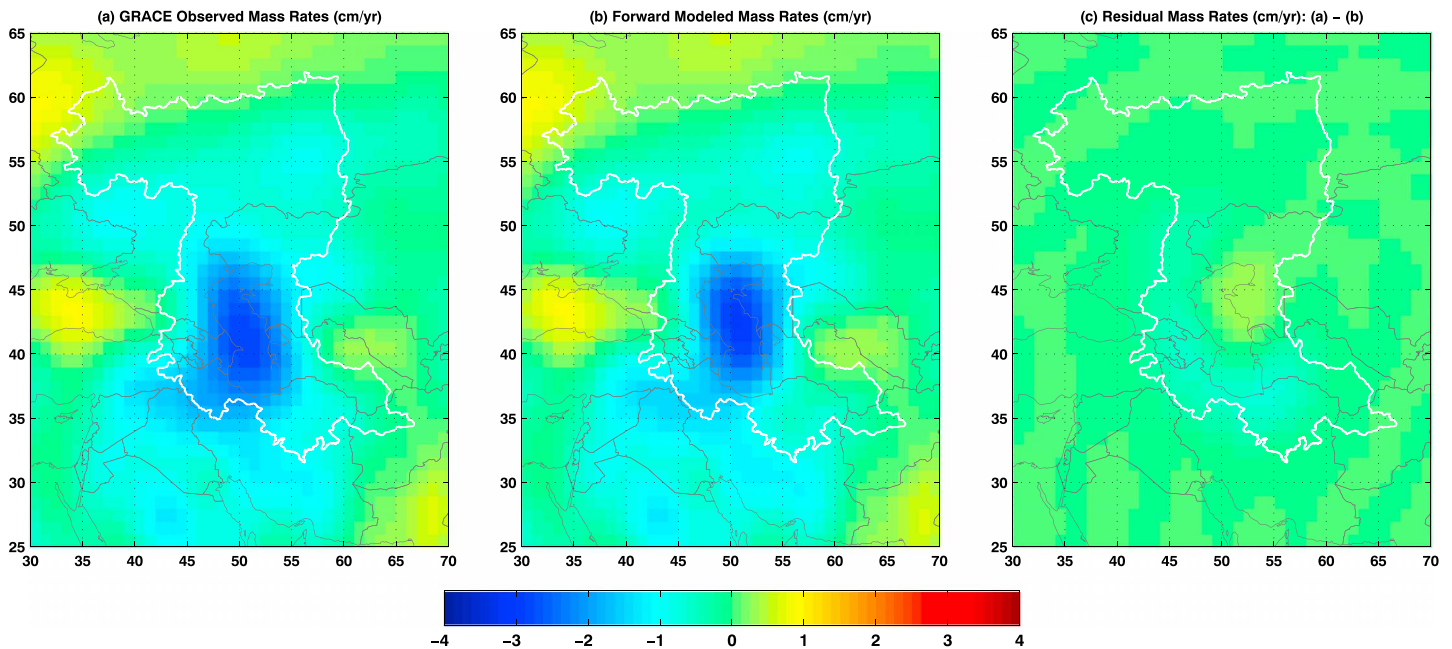


**Figure 3.** (a) GRACE mass rates (in cm/yr of equivalent water height) in the Caspian Sea and surrounding regions, after 300 km Gaussian smoothing (no decorrelation filtering is applied). (b) Constrained forward model predicted mass rates after the same 300 km Gaussian smoothing. (c) Residuals between GRACE observations and constrained forward model predicted mass rates, i.e., Figures 3a and 3b. The Caspian Sea drainage basin is circled by the white contour line.

[Chen *et al.*, 2015], the average Caspian Sea rate (April 2002 to April 2015) is about  $-6.67$  cm/yr (or  $-24.6$  Gt/yr) (Figure 4a). Figure 4b shows the evolution of RMS differences between GRACE observations and predictions from the forward modeled mass rate. There is rapid convergence, and after six or seven iterations, the residual over the entire Caspian Sea is below 0.8 Gt/yr or about 3% of the total signal,  $-24.6$  Gt/yr. The GRACE apparent mass rate is about 36% of the forward model estimate ( $2.40/6.67 = 0.36$ ).

The Caspian Sea region is largely arid, except for northern Volga and Ural basins, so TWS changes in surrounding areas are relatively small, with annual peak-to-peak changes of a few cm, much smaller than the 40 cm variations within the Caspian Sea [Humphrey *et al.*, 2016]. Therefore, we assume that seasonal and longer time scale variations in GRACE estimates are subject to the same leakage bias ratio determined for mass rates (36% or  $2.40/6.67$ ), and we adjust the GRACE Caspian Sea level change time series by the reciprocal ( $6.67/2.4$ ) to remove the bias. This adjusted time series is plotted in Figure 5a, together with smoothed GRACE SH estimates (300 km Gaussian smoothing) without the leakage bias correction (with and without p4m6 decorrelation filtering). In the p4m6 decorrelation filtering, for SH orders 6 and above, a degree 4 polynomial is fitted by least squares and removed from even and odd coefficient pairs. Having now reviewed the treatment of leakage to be applied, we now treat the GRACE products to be intercompared both with and without this correction, which is henceforth abbreviated with “LC.”

### 2.3. GRACE Mascon Estimates

GRACE mascon estimates are alternative GRACE mass change solutions. The mascon method largely mitigates the effects of stripping that are so pronounced in the SH solutions. GRACE mascon solutions do not require Gaussian smoothing or decorrelation filtering. They should offer improved spatial resolution [Save *et al.*, 2012, 2016; Watkins *et al.*, 2015]. Two GRACE mascon estimates of Caspian Sea mass variations are examined here. The first is the NASA Jet Propulsion Laboratory (JPL) version 2 mascon solution, which uses a direct approach, with the range data reckoned to mass changes of perturbing spherical caps [Vins *et al.*, 2011], and is constrained by a priori information derived from near-global geophysical models to prevent striping in the solutions [Watkins *et al.*, 2015; Wiese, 2015]. JPL mascon (JPL MC) solutions are first obtained on  $3^\circ \times 3^\circ$  equal area grids. Each  $3^\circ \times 3^\circ$  element is then resampled at  $0.5^\circ \times 0.5^\circ$ . Scale factors calculated from TWS estimates of the Community Land Model (CLM 4.0) [Oleson *et al.*, 2010] are separately provided and can be used to infer spatial variations among the  $0.5^\circ \times 0.5^\circ$  subelements within each  $3^\circ \times 3^\circ$  element (note that there are 36

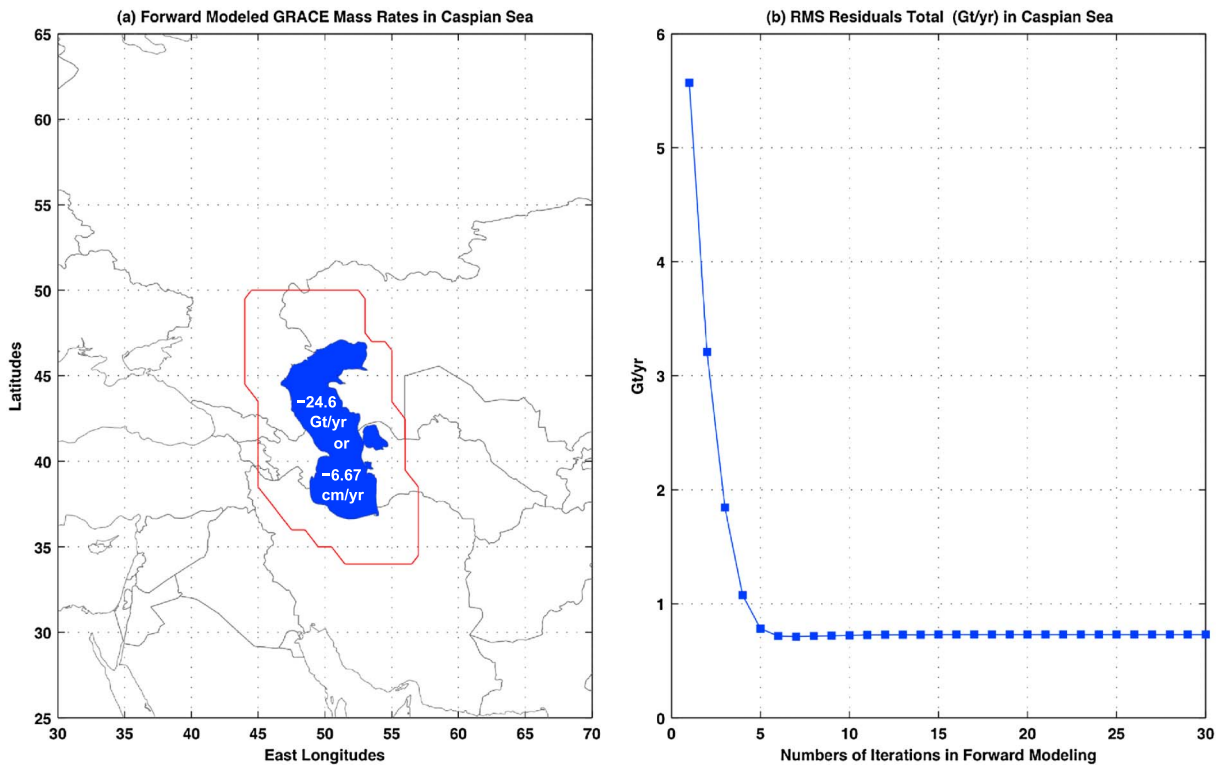


**Figure 4.** (a) Constrained forward modeled true mass rate in the Caspian Sea,  $-24.6$  Gt/yr (or  $-6.67$  cm/yr of equivalent water height). The true mass rates on grids outside the region circled by the red contour line are set to unsmoothed GRACE results. (b) Total RMS residuals (in Gt/yr) between GRACE observations and constrained forward model predicted mass rates, as a function of iterations in forward modeling experiments.

$0.5^\circ \times 0.5^\circ$  subelements within each equal area  $3^\circ \times 3^\circ$  mascon element at the equator, and many more than 36 at higher latitudes). In order to reduce spatial leakage from land to oceans, a coastline resolution improvement (CRI) filter is applied [Wiese, 2015; Wiese et al., 2016]. Monthly JPL MC CRI version 2 (CRIv02) solutions over the same April 2002 to April 2015 period are used to compute mean Caspian Sea level change, as shown in Figure 5b.

The CSR mascon (CSR MC) solution is based on regularization method [Save et al., 2012] and derived entirely from GRACE information without any input from external models and, unlike the JPL solution, is independent of TWS or other geophysical models [Save et al., 2016]. CSR mascon solutions are computed on an equal area geodesic grid composed of hexagonal tiles approximately 120 km wide or roughly  $1^\circ \times 1^\circ$  at the equator. Each mascon cell is related to the range-rate observations via partials with respect to SH expansion, truncated to degree and order 120. Mass anomalies in each mascon are computed from satellite range-rate observations via their partial derivatives [Save et al., 2016; Scanlon et al., 2016]. Constraints on the solution include separation of land and ocean signals to reduce leakage (by producing an intermediate mascon solution), forward modeling of annual and trend signals from ice losses in polar regions and mountain glaciers to avoid overconstraining the GRACE solution, and application of a time-variable regularization matrix for mascon estimation [Save et al., 2016]. Like the JPL solution, the CSR MC is also provided on a  $0.5^\circ \times 0.5^\circ$  grid. The CSR MC-derived Caspian Sea level change time series is shown in Figure 5b.

Apparently, both JPL and CSR mascon Caspian Sea level change estimates are also affected by leakage error. Even though both mascon estimates show relatively larger magnitudes than the GRACE SH 300 km results, they are significantly smaller than the leakage-corrected SH estimates (i.e., the forward modeled results) and altimeter observations (see Figure 5). We show in Figure 6a the long-term mass rates in the Caspian Sea and surrounding regions derived from the JPL MC solutions (on  $0.5^\circ \times 0.5^\circ$  grids) over the period of April 2002 to April 2015. The CLM 4.0 TWS scale factors were not applied in our calculations (as our focus here is on Caspian Sea level rather than TWS change). Clearly, the original  $3^\circ \times 3^\circ$  mascons do not separate mass changes between the Caspian Sea and surrounding land because the geophysical placement of the

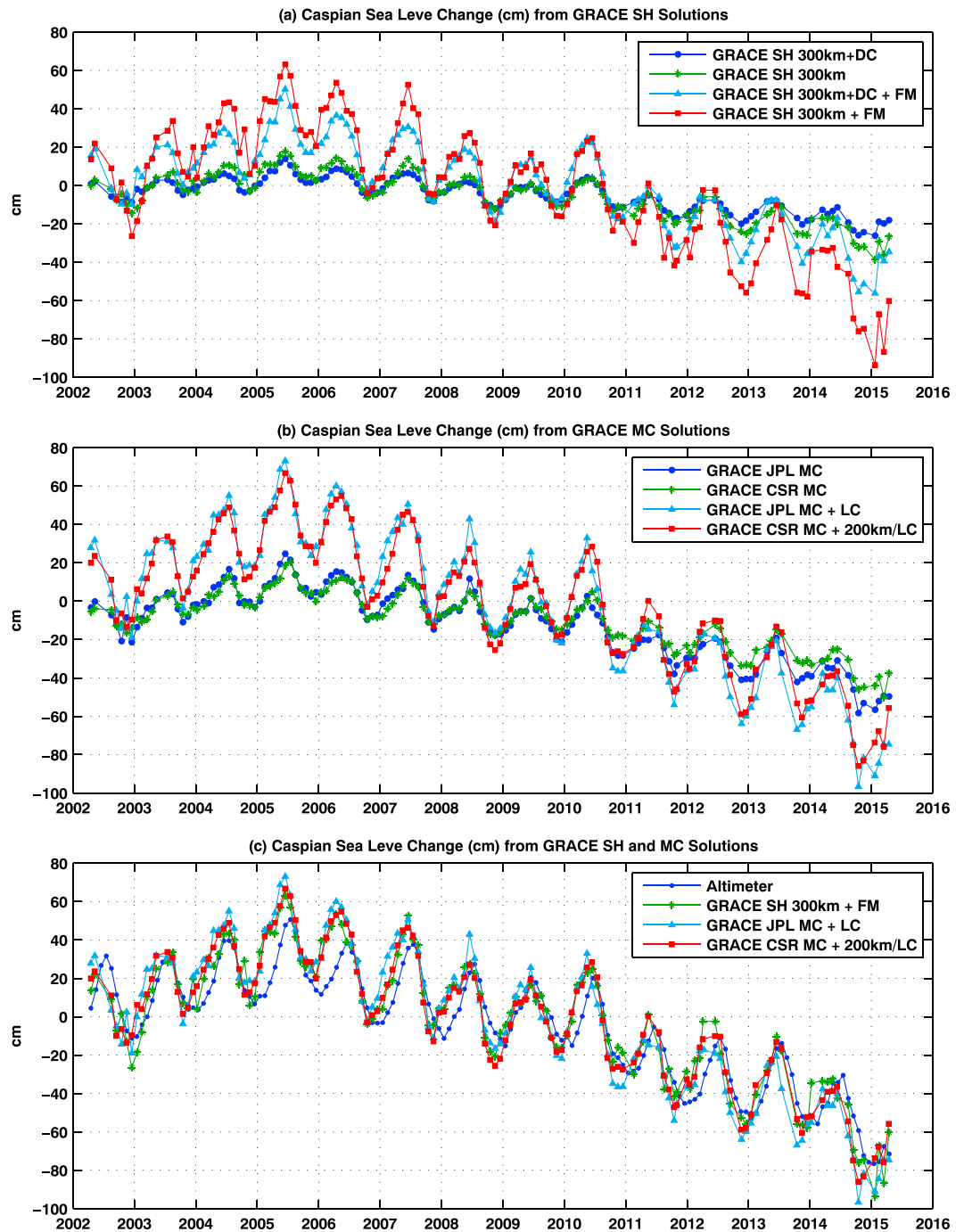


**Figure 5.** GRACE monthly Caspian Sea level change time series from different data processing methods and GRACE solutions. (a) Four SH series are derived from CSR RL05 with 300 km Gaussian smoothing: decorrelation filtered (300 km + DC); Gaussian smoothed only (300 km), forward modeling with decorrelation filtering and leakage correction (300 km + DC + FM) and with leakage correction (300 km + FM). (b) Four mascon time series are from the JPL CRIV02 and CSR regularized mascon solutions without and with leakage corrections (LCs). A 200 km buffer zone is used in CSR MC leakage correction here. (c) Leakage-corrected GRACE SH and mascon time series, compared with altimeter observations.

mascon boundaries does not coincide with the outline of the Caspian Sea and there is no information provided at submascon spatial scales from GRACE. Without a priori information as constraints, GRACE's capability of separating mass changes on the Earth surface is also controlled by the fundamental limitations of GRACE spatial resolution (set by altitudes of and distance between the two satellites). A practical (approximate) way

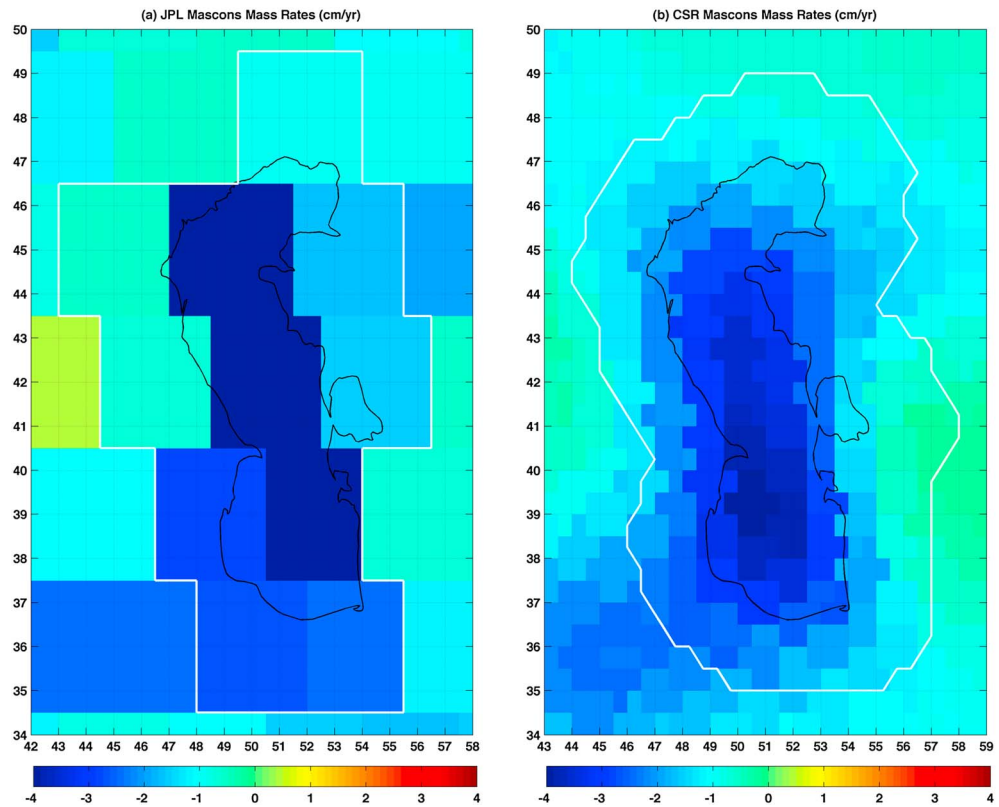


**Figure 6.** (a) JPL mascon mass rates (in cm/yr of equivalent water height) in the Caspian Sea and surrounding regions. All  $3^{\circ} \times 3^{\circ}$  equal area mascons that overlap or partly overlap with the Caspian Sea are circled by the white lines. (b) CSR mascon mass rates (cm/yr) in the Caspian Sea and surrounding regions. All  $0.5^{\circ} \times 0.5^{\circ}$  mascons that are within 200 km from the coast of the Caspian Sea are circled by the white curves.

to correct leakage error in JPL MC Caspian Sea estimates is to sum up mass changes in all original  $3^{\circ} \times 3^{\circ}$  mascons (circled by white lines in Figure 6a) and assign these totals to the Caspian Sea. Certainly, some of the variations (within all these  $3 \times 3$  mascons) may come from TWS variations, but these can be removed by using estimates from land surface model (LSM). Taking this approach, we compute leakage-corrected Caspian Sea mass change from the JPL MC solutions and show the results in Figure 5b, to compare with the mascon estimates before leakage correction.

Figure 6b shows CSR MC long-term mass rates in the same region and over the same period (April 2002 to April 2015). Leakage of Caspian Sea mass change into surrounding land regions is also evident. Since the actual dimension of tiles used in the CSR mascon estimation is roughly 120 km, depending on the signal and the area of interest, it is advisable to extend the study region for basin analysis by roughly 120 km–200 km outside the desired region in order to account for the possibility that part of mascon tile is residing outside the study region. To correct this leakage error, we have included all  $0.5^{\circ} \times 0.5^{\circ}$  mascons within 200 km from the coast of the Caspian Sea (i.e., within the region circled by the white contour line in Figure 6b) and reallocated the totals back into the Caspian Sea to get the leakage-corrected CSR MC estimates (see Figure 5b). This is consistent with the fact that the regularization constraint in CSR mascon solutions uses information from a 200 km Gaussian smoothed regularized SH solutions from GRACE [Save *et al.*, 2016]. The three leakage-corrected GRACE estimates (SH 300 km + FM, JPL MC + LC, and CSR MC + LC) and satellite altimeter observations are shown in Figure 5c. We show in Table 1 the amplitudes and phases of annual and semiannual variations and linear rates of different GRACE estimates of Caspian Sea mass change by using unweighted least squares fit, compared with those from altimeter observations and other effects discussed later.

**2.4. Steric Effect on Caspian Sea Level Change**

Water temperature and salinity variations may cause steric changes in Caspian Sea level that would not be observed by GRACE. We lack temperature and salinity data to directly compute steric changes in the

**Table 1.** Amplitudes and Phases of Annual and Semiannual Components of Caspian Sea Level Change From Satellite Altimeter Observations and GRACE Estimates for the Period of April 2002 to April 2015<sup>a</sup>

Caspian Sea Level	Annual		Semiannual		Linear Trend (cm/yr)
	Amplitude (cm)	Phase (deg)	Amplitude (cm)	Phase (deg)	
Altimeter observation	17.6 ± 1.4	266 ± 5	3.3 ± 1.4	69 ± 25	-6.07 ± 0.26
GRACE SH 300 km + FM + steric – TWS	17.5 ± 2.0	272 ± 6	4.2 ± 2.0	78 ± 27	-6.00 ± 0.39
GRACE JPL MC (+LC) + steric – TWS	20.1 ± 2.0	274 ± 6	5.4 ± 2.0	81 ± 21	-7.19 ± 0.39
GRACE CSR MC (+SF/LC) + steric	16.2 ± 1.9	270 ± 5	6.2 ± 1.8	80 ± 17	-6.29 ± 0.35
GRACE CSR MC (+200 km/LC) + steric – TWS	21.0 ± 1.9	270 ± 5	6.3 ± 1.8	79 ± 16	-6.08 ± 0.34
GRACE CSR MC (+100 km/LC) + steric – TWS	16.5 ± 1.5	264 ± 5	5.2 ± 1.5	79 ± 16	-5.06 ± 0.28
GRACE SH 300 km + FM	18.7 ± 2.1	300 ± 6	4.5 ± 2.1	80 ± 26	-6.70 ± 0.40
GRACE SH 300 km	6.7 ± 0.8	300 ± 6	1.6 ± 0.7	80 ± 26	-2.41 ± 0.14
GRACE SH 300 km + DC + FM	14.7 ± 1.3	313 ± 5	3.4 ± 1.3	82 ± 22	-4.49 ± 0.25
GRACE SH 300 km + DC	5.6 ± 0.5	313 ± 5	1.3 ± 0.5	82 ± 22	-1.69 ± 0.09
GRACE JPL MC + LC	21.2 ± 2.0	310 ± 6	5.2 ± 2.0	81 ± 23	-8.15 ± 0.40
GRACE JPL MC	9.6 ± 1.1	297 ± 6	3.0 ± 1.1	78 ± 20	-3.89 ± 0.21
GRACE CSR MC + 200 km/LC	20.9 ± 1.9	305 ± 5	6.1 ± 1.9	77 ± 17	-7.16 ± 0.36
GRACE CSR MC + SF/LC	16.9 ± 1.9	290 ± 6	6.2 ± 1.9	77 ± 17	-6.20 ± 0.35
GRACE CSR MC	8.2 ± 0.9	291 ± 6	3.0 ± 0.9	79 ± 17	-3.01 ± 0.17
Steric effect	6.0 ± 0.0	184 ± 0	0.04 ± 0.0	155 ± 0	-0.09 ± 0.0
TWS leakage (w/ FM)	2.9 ± 0.3	17 ± 6	0.3 ± 0.3	103 ± 47	-0.78 ± 0.05
TWS leakage (w/o FM)	0.8 ± 0.1	17 ± 6	0.1 ± 0.1	103 ± 47	-0.21 ± 0.01
TWS leakage (JPL MC + LC)	7.1 ± 0.3	28 ± 3	0.2 ± 0.3	237 ± 93	-1.05 ± 0.06
TWS leakage (CSR MC + 200 km)	6.9 ± 0.3	30 ± 3	0.2 ± 0.3	299 ± 106	-1.17 ± 0.06
TWS leakage (CSR MC + 100 km)	3.5 ± 0.2	34 ± 3	0.1 ± 0.2	311 ± 111	-0.54 ± 0.03

<sup>a</sup>Phase  $\phi$  is defined for the annual term as  $\sin(2\pi(t - t_0) + \phi)$ , where  $t_0$  refers to  $h^0$  on 1 January and similarly for the semiannual term.

Caspian Sea. As an alternative, we use analogue measurements of ocean temperature and salinity changes in Northern Atlantic over the same latitude range from the Array for Real-Time Geostrophic Oceanography (ARGO) float network [Roemmich and Owens, 2000; Argo, 2000] to approximate possible steric effect on the Caspian Sea level change. Temperature is a dominant control on steric sea level change, and steric sea level change of the world ocean exhibits strong zonal patterns [Chen et al., 2000]. But, due to the distinctively different geographical locations and expected different thermal heating processes between the Caspian Sea and Northern Atlantic, this analogue analysis may be only a first-order approximation of the likely magnitude and phase of the steric effect in the Caspian Sea. Global gridded ARGO data from January 2004 through December 2014, provided by the Scripps Institution of Oceanography at the University of California at San Diego ([http://www.argo.ucsd.edu/Gridded\\_fields.html](http://www.argo.ucsd.edu/Gridded_fields.html)), were used to compute average steric sea level changes in Northern Atlantic (37°N to 47°N). Before 2004, ARGO float coverage is too sparse to provide meaningful global grids. Annual variation and linear trend were estimated by using unweighted least squares and shown in Table 1 and Figure 7.

### 2.5. Hydrologic Effects on GRACE Estimates

TWS changes in regions surrounding the Caspian Sea are expected to be small due to the relatively arid climate noted earlier [Humphrey et al., 2016]. Time series in Figure 5 were computed, assuming these surrounding TWS variations are zero. However, we can use TWS estimates from the Global Land Data Assimilation System (GLDAS) to test this assumption. GLDAS ingests satellite- and ground-based observations and employs advanced land surface modeling and data assimilation techniques, to estimate land surface states and fluxes [Rodell et al., 2004]. The GLDAS TWS estimates used here are from the Noah (National Centers for Environmental Prediction/Oregon State University/Air Force/Hydrologic Research Lab Model) LSM [Ek et al., 2003]. They include variations of soil moisture from the top 2 m of soil and water equivalent snow depth and cover the same period as the GRACE data.

We express GLDAS TWS grids in an SH expansion and compute mass change grids from the expansion, truncated at degree and order 60, with 300 km Gaussian smoothing. A first-order estimate of leakage effects is the average of GLDAS TWS variations over the Caspian Sea. However, this may represent only a portion of leakage in constrained forward modeling results because the forward modeling process moves signal from

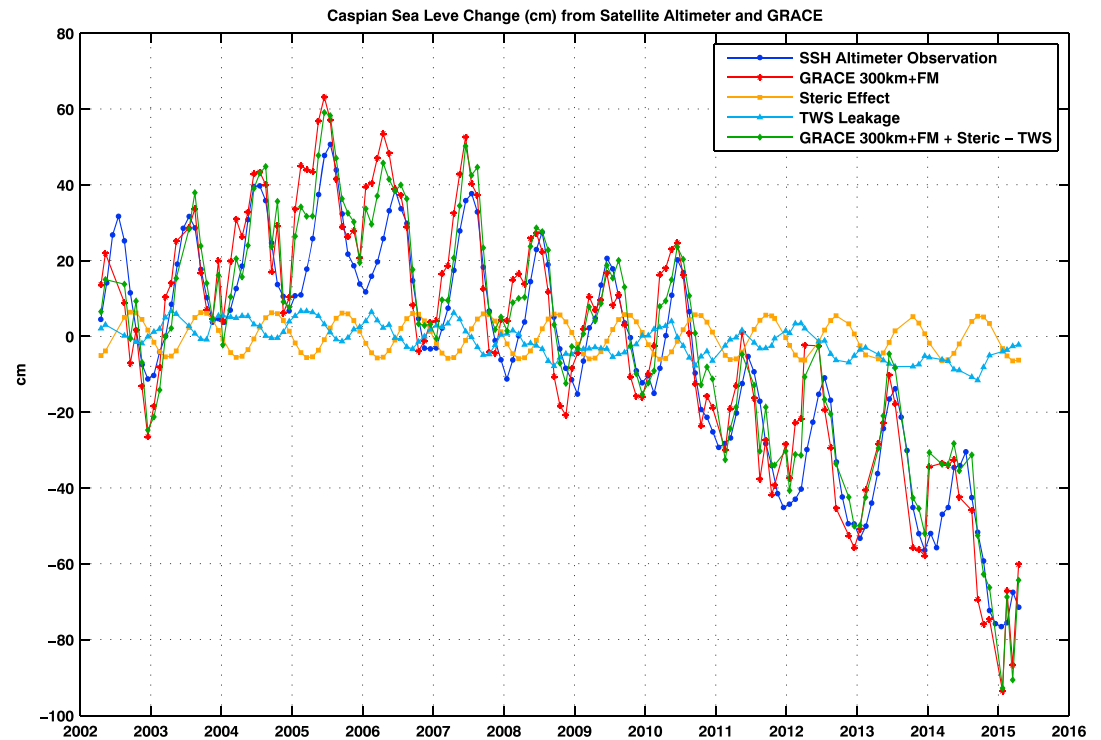


**Figure 7.** Monthly Caspian Sea level changes from satellite altimeter observations and GRACE CSR RL05 SH solutions with 300 km Gaussian smoothing and forward modeling leakage correction (300 km + FM), without or with steric and TWS correction. Separate estimates of steric and terrestrial water storage (TWS) leakage effects are superimposed for comparisons.

surrounding regions into the Caspian Sea (see Figures 3 and 4). We use forward modeled GRACE results to compute a scale factor that estimates this effect and apply it to the GLDAS TWS average over the Caspian Sea. This is an estimate of TWS leakage effects for forward model estimates. For SH estimates without forward modeling, average GLDAS TWS over the Caspian Sea is taken as the estimate. Figure 7 shows that the GLDAS estimates of TWS effects are relatively small in magnitude and show dominantly seasonal variations. The lack of a large trend supports the assumption of zero TWS contamination used in the earlier forward modeling estimates of mass rates. For the two GRACE (leakage-corrected) mascon estimates, TWS contributions are directly computed from all GLDAS TWS grids (without any SH truncation or spatial filtering) within the involved mascon tiles (i.e., within the areas circled by the white contour lines in Figures 6a and 6b).

## 2.6. Lake Height Changes From Satellite Altimeter

Methods of calibrating lake height (level) changes from satellite altimeter have been extensively reported in the literature since the mid-90s [Birkett, 1995]. Since 2003, a Web service called Hydroweb (<http://hydroweb.theia-land.fr/>) has been providing time series of water height changes from satellite altimetry in an automatic near real-time algorithm for the largest lakes in the world. For the Caspian Sea, different satellite tracks were used to calculate the mean water height by using data sets from TOPEX/Poseidon, Jason-1, Jason-2, Geosat Follow-On, Envisat, and SARAL (Satellite with ARGOS and ALtiKa) [Cretaux *et al.*, 2016].

It is, however, needed to correct biases in the altimeter measurements due to geoid error between two tracks and due to instrumental biases of different altimeters. Both types of error are corrected by calculating a priori intertrack and removing intersatellite biases. For large lakes like the Caspian Sea, an along-track geoid correction, which must be applied to each range measurement, is calculated by using the so-called “repeat track technique” [Birkett, 1995; Cretaux *et al.*, 2016]. The geoid errors from classical models can reach up to few dozens of centimeters like over the Lake Issykkul [Cretaux *et al.*, 2009]. In the case of having several tracks of the same satellite covering the lake, the geoid slope between two different tracks is calculated by computing the

slope for each track separately, and then calculating relative biases among different tracks. A full description of the altimetry data processing for lakes is provided in *Cretaux et al.* [2016].

### 3. Results and Discussion

There are notable differences among the four different GRACE SH estimates of Caspian Sea level change in Figure 5a, in both amplitudes of seasonal variations and longer time scale changes. For example, GRACE 300 km + DC + FM shows that decorrelation filtering has attenuated both seasonal and longer term variations relative to GRACE 300 km + FM. This is due to the north-south orientation of the Caspian Sea. Similar attenuation is evident when comparing GRACE 300 km + DC with GRACE 300 km curves. Among the four SH estimates, GRACE 300 km + FM shows the largest variations.

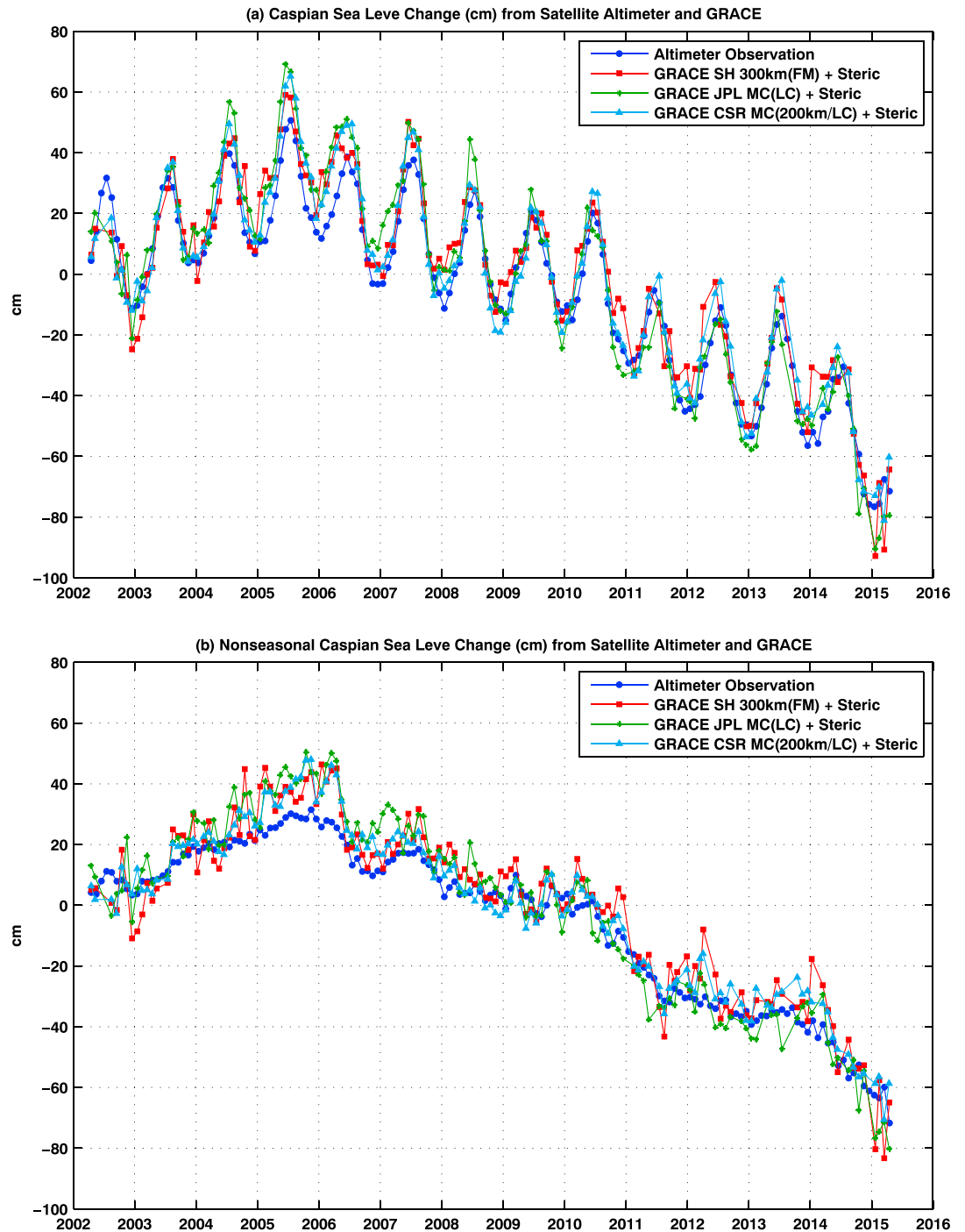
Without leakage corrections, the two mascon estimates (GRACE JPL MC and CSR MC) show larger variations than SH estimates (300 km + DC and 300 km), confirming that mascon solutions are subject to less leakage error than conventional SH solutions. JPL MC (CRLv02) variations are somewhat larger than CSR MC, but both are considerably smaller than forward modeled GRACE SH estimates. However, the two leakage-corrected mascon estimates (JPL MC + LC and CSR MC + LC) agree well with forward modeled SH estimates (300 km + FM) and altimeter observations (see Figure 5c), although the altimeter time series shows a slight phase difference in seasonal variations compared to GRACE estimates.

Figure 7 shows GLDAS TWS leakage predicted for forward model estimates and ARGO steric estimates. GRACE SH forward modeled (300 km + FM) results are shown, with a separate curve after steric and TWS leakage corrections are applied. Application of steric and TWS leakage corrections results in relatively minor changes. With or without these corrections, GRACE forward modeled results agree well with altimeter observations (Figure 7, blue curve) at both seasonal and longer time scales. The slight seasonal phase difference between red (GRACE 300 km + FM, uncorrected) and blue curves is reduced by adding estimated TWS and steric corrections (green curve).

The CSR MC solutions are believed to have an inherent 200 km smoothing built, considering the fact that the regularization matrix used in CSR MC solutions is based on 200 km Gaussian smoothed GRACE SH solutions [Save et al., 2016]. We carry out some additional experiments to estimate potential leakage bias in CSR MC estimates of CSL changes from a completely different approach via scale factor [Landerer and Swenson, 2012]. We construct a mass change model in the Caspian Sea and surrounding regions by combining monthly GLDAS TWS changes over land and altimeter SSH changes over the Caspian Sea. Following the similar procedures as in Landerer and Swenson [2012], we convert the mass model into gravity SH coefficients, and then estimate CSL changes from the converted gravity SH coefficients with truncation at degree and order 60 and 200 km Gaussian smoothing. A scale factor is estimated as the average ratio between the original altimeter SSH change and the 200 km Gaussian smoothed results via minimizing the RMS of the residuals. The estimated scale factor (~2.06) is then applied to CSR MC estimates to get the leakage-corrected CSR MC estimates. For the simplicity and clarity of the comparisons, the scale factor leakage-corrected (noted as SF/LC) time series are not included in related comparisons (Figure 8). We only provide the amplitudes and phases of annual and semiannual variations and linear trend estimated from unweighted least squares fit in Table 1 for comparisons.

Figure 8a compares the altimeter series with three GRACE estimates (300 km + FM, JPL MC + LC, and CSR MC + LC) all corrected for leakage, steric, and TWS effects. Figure 8b compares the same series after annual and semiannual sinusoidal components were removed from all series. All three GRACE estimates agree remarkably well with altimeter observations, at both seasonal and longer time scales. With steric and TWS corrections, the slight seasonal phase difference between GRACE estimates and altimeter observations (shown in Figure 5c) is notably reduced. Table 1 quantifies this, showing amplitudes and phases of (unweighted least squares fit) annual and semiannual coefficients and linear rates. The results from GRACE SH (300 km + FM) and two mascon solutions (JPL MC and CSR MC) are highlighted in blue bold fonts. These can be compared with altimeter values (black bold fonts). The CSR MC estimates with 100 km buffer zone are also included for comparisons.

We do see an apparent separation of ~10 cm between altimetry observations and GRACE measurements (with steric and TWS corrections) between the end of summer 2004 and the beginning of summer 2006 (see



**Figure 8.** (a) Monthly Caspian Sea level changes from satellite altimeter observations and different GRACE estimates from different data processing methods or products. Approximate seasonal and long-term steric effects have been added to GRACE estimates, in order to compare with altimeter observations. TWS leakage corrections have also been applied to GRACE estimates. (b) Same as Figure 8a but with annual and semiannual variations removed from all series.

Figure 8b). The exact reasons for this discrepancy are unknown. Given the rather large magnitude of this bias, the uncertainty in estimated TWS and steric effects is unlikely the major cause. The altimeter calibration error,  $\sim \pm 8.5$  cm during this period (see Figure 2), may play a role here, and same as the error in GRACE estimates, especially due to leakage corrections.

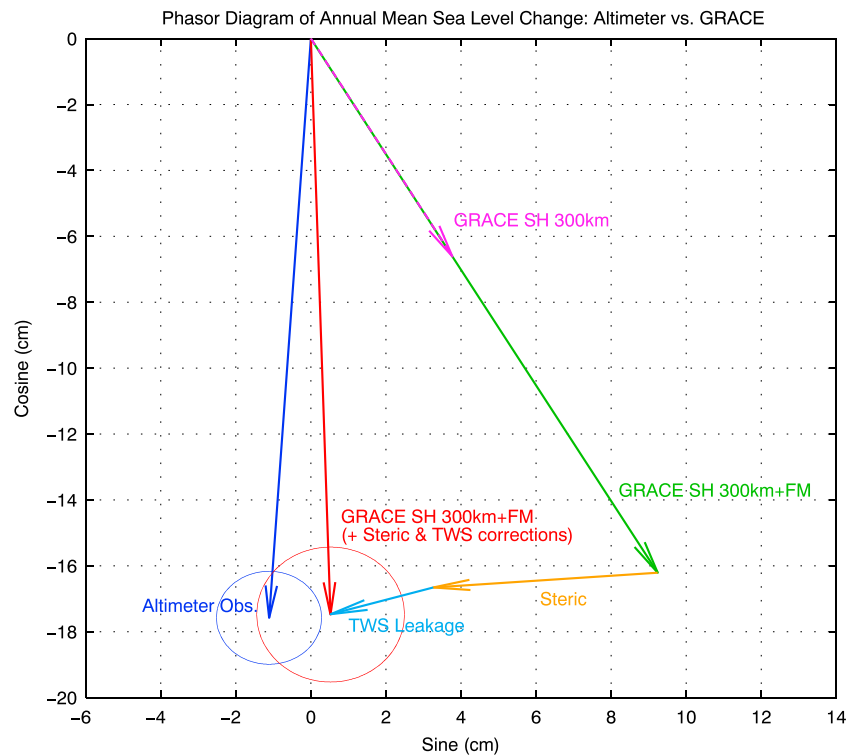


**Figure 9.** Phasor diagram of annual Caspian Sea level changes from satellite altimeter observations and GRACE CSR RL05 SH solutions with 300 km Gaussian smoothing and forward modeling leakage correction (300 km + FM) and steric and TWS leakage corrections. Uncertainties of altimeter and GRACE (with all corrections) annual components are shown by the blue and red ellipses, respectively.

Table 1 shows that GRACE SH (300 km + FM + steric – TWS) variations are in complete agreement with satellite altimeter results for both seasonal terms and the linear trend. Annual amplitudes and phases agree within formal errors ( $17.5 \pm 2.0$  cm versus  $17.6 \pm 1.4$  cm and  $272 \pm 6$  degrees versus  $266 \pm 5$  degrees). There is similar agreement for linear trends ( $-6.00 \pm 0.39$  cm/yr versus  $-6.07 \pm 0.26$  cm/yr). Both mascon results show considerably larger seasonal amplitudes than the altimeter and GRACE SH estimates, although the CSR MC (200 km + steric – TWS) shows virtually the same linear trends as seen from altimeter ( $-6.08 \pm 0.34$  cm/yr versus  $-6.07 \pm 0.26$  cm/yr).

Inclusion of ARGO-like steric and GLDAS TWS corrections has improved the agreement between GRACE and altimeter results at both seasonal and long-term time scales. This is evident in Table 1 and in Figure 9. While the two corrections can only be considered approximate, both added to the GRACE 300 km + FM annual vector bring it closer to the altimeter annual phasor. The remaining difference would nearly disappear, if the steric estimate were amplified by about 20 to 30%. Figure 9 also indicates that annual phase differences between altimeter and GRACE forward modeled estimates (300 km + FM) are unlikely to arise from errors associated with forward modeling because these changes only signal amplitude, not phase. If ARGO steric and GLDAS TWS annual phases are about right, then the GRACE forward modeled annual component appears to be reasonably accurate. Similar annual phasor diagrams for the three mascon estimates (JPL MC + LC, CSR MC + 200 km/LC, and CSR MC + SF/LC) are shown in Figure 10 (the results from CSR MC SF/LC are also included in the phasor diagram for comparisons).

After steric and TWS leakage corrections, the two mascon results with buffer zone LC (JPL MC/LC and CSR MC 200 km/LC) show similar annual amplitudes, which are about 3 cm larger than the altimeter result. For the same reasons discussed above, the discrepancy between altimeter and these GRACE mascon's seasonal variations is more likely due to error in mascon estimates. However, the CSR MC estimates via scale factor approach (i.e., CSR MC SF/LC) show substantially smaller annual amplitude than that from the 200 km buffer zone approach (i.e., CSR MC 200 km/LC) and agree better with altimeter observations ( $16.2 \pm 1.9$  cm versus  $17.6 \pm 1.4$  cm). The

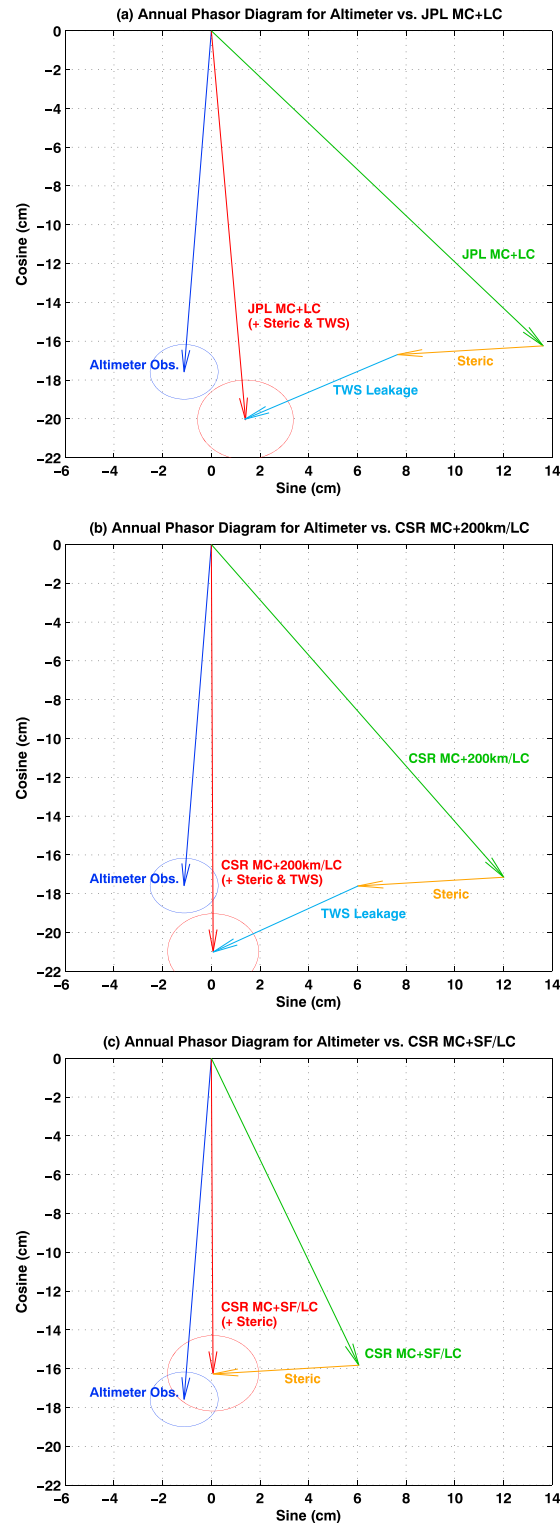


**Figure 10.** Phasor diagram of annual Caspian Sea level changes from satellite altimeter observations and (a) JPL MC + LC, (b) CSR MC + 200 km/LC, (c) CSR MC + SF/LC. ARGO-like steric effect and TWS leakage corrections are also included. In CSR MC SF/LC (scale factor/leakage correction) estimate, TWS effect has already been implemented in the simulations. Uncertainties of altimeter and GRACE (with all corrections) annual components are shown by the blue and red ellipses, respectively.

comparisons between the three CSR MC estimates (with 200 km or 100 km buffer zone, or scale factor) appear to suggest that the 200 km buffer zone might have led to overestimation of seasonal variations of Caspian Sea mass change. Using a smaller buffer zone is expected to reduce the seasonal variation but may lead to underestimation of linear trend at the same time. The scale factor-based CSR MC estimates show improved agreement with altimeter SSH measurements, but notable discrepancy still exists, especially at seasonal time scales. The JPL MC estimates (with leakage, steric, and TWS effects corrected) show the largest linear trend ( $-7.19 \pm 0.39$  cm/yr).

#### 4. Conclusions

Satellite radar altimeter observations show that Caspian Sea level has been declining at a rate of  $-6.07 \pm 0.26$  cm/yr with superimposed annual fluctuations of amplitude  $17.6 \pm 1.4$  cm, over the period of April 2002 to April 2015. These create a large mass change signal in a well-defined geographical location surrounded by mostly arid basins. Both signal amplitude and geography provide a unique opportunity to evaluate various GRACE solutions and processing methods.

All GRACE solutions examined here show seasonal and long-term variations that are qualitatively consistent with the altimeter data. However, excellent quantitative agreement is obtained only when GRACE estimates are corrected for spatial leakage into surrounding areas. All other estimates show variations with smaller magnitudes, a bias expected to accompany spatial leakage into the surrounding arid region. While with appropriate leakage corrections, both GRACE SH and MC estimates agree well with altimeter and the GRACE SH estimates with leakage correction via forward modeling show the best agreement with

altimeter observations. This appears to be understandable, as from a mathematical point of view, leakage error in GRACE SH solutions can be satisfactorily removed, as long as geographical locations of the mass changes are known and other errors can be removed separately [Chen *et al.*, 2015]. The relatively large discrepancy between mascon results and altimeter SSH measurements is mainly because the definition of the mascon boundaries does not coincide with the outline of the Caspian Sea. Specially solved constrained mascon solutions by using the Caspian Sea's geographical information are expected to show substantially small leakage bias.

There is a similar bias when the decorrelation filter is used, consistent with the purpose of this filter to suppress longitudinal noise stripes, and its collateral effect on signals with a north-south orientation, such as Caspian Sea level changes. We estimate that steric effects are a minor component of Caspian Sea level change. ARGO-like results from the North Atlantic likely have about the correct annual phase. Agreement between GRACE and altimeter results would be improved if Caspian Sea annual steric effects were slightly larger than the ARGO estimate. The GLDAS estimate of TWS leakage reduces the remaining annual phase difference and contributes about 10% to the GRACE linear trend rate (Table 1).

Removal of leakage error is demonstrated to be a critical GRACE postprocessing element. For SH solutions which involve linear filtering methods such as SH truncation and Gaussian smoothing, there are logical postprocessing approaches such as forward modeling [Chen *et al.*, 2015] or application of scale factors [Landerer and Swenson, 2012]. Although mascon solutions are free of longitudinal stripe noise and show less leakage error than SH solutions, they still suffer from spatial leakage biases. Without leakage corrections, both JPL and CSR mascon biases lead to amplitude reductions of about 50% relative to altimeter or leakage-corrected GRACE SH signals.

We have demonstrated, via excellent agreement between leakage-corrected GRACE estimates and the altimeter record, a validation and assessment of GRACE processing methods. In combination, GRACE and altimeter data provide information concerning steric changes, an integrated measure of temperature (and related heat content) and salinity changes, of which heat content change plays a dominant role. Both validation of GRACE and information about steric (or heat content) variations have been goals pursued in global ocean studies, but the unique features of the Caspian Sea, isolated geography, arid surroundings, and large signals, allow these goals to be realized. Unlike the global ocean with decent coverage by the ARGO network, there are no adequate in situ temperature and salinity measurements over the Caspian Sea and global ocean circulation models do not cover this enclosed sea either. The comparisons between GRACE and altimeter data offer a unique means for studying heat content (and salinity) change of the Caspian Sea.

The large seasonal Caspian Sea level variations are mainly driven by seasonal fluctuations of precipitation and evaporation over the Caspian Sea and river discharge from surrounding drainage basins. The long-term decrease of the Caspian Sea level over the last decade is believed to reflect the imbalance between water inflow (from precipitation and river discharge) and outflow. Our additional analysis based on climate model estimates suggests that increased yearly evaporation rates over the Caspian Sea during the last 10 years appear to have played a major role in causing the Caspian Sea level decrease. Interannual variations of the Caspian Sea level are likely related to precipitation anomalies in Caspian drainage basin controlled by the Arctic Oscillation [Matsuo and Heki, 2012]. Detailed analysis on geophysical interpretation of Caspian Sea level is beyond the scope of the present study, which focuses on the validation of GRACE-observed mass variations over the Caspian Sea by using satellite altimeter measurements.

### Acronyms

The following acronyms and abbreviations are used in this paper.

ARGO	Array for Real-Time Geostrophic Oceanography
CSR	Center for Space Research
GLDAS	Global Land Data Assimilation System
GFO	Geosat Follow-On
GRACE	Gravity Recovery and Climate Experiment
JPL	Jet Propulsion Laboratory
LC	leakage correction
LSM	land surface model
Mascon	mass concentration

MC	mascon
Noah	National Centers for Environmental Prediction/Oregon State University/Air Force/Hydrologic Research Lab Model
SARAL	Satellite with ARgos and ALtiKa
SF	scale factor
SH	spherical harmonic
SSH	sea surface height
TWS	terrestrial water storage

### Acknowledgments

We are grateful to Erik R. Ivins and Kosuke Heki for their comprehensive and insightful reviews that led to improved analysis and presentation of the results. This study was supported by the NASA GRACE Science Team Program (NNX12AJ97G), the NASA ESI Program (NNX12AM86G and NNX17AG96G), and the NASA GRACE and GRACE Follow-On projects (under contract NNL14AA00C and JPL subcontract 1478584). GRACE RL05 gravity solutions are provided by the GRACE Science Team (<ftp://podaac-ftp.jpl.nasa.gov/allData/grace/>). JPL mascon solutions are available at <ftp://podaac.jpl.nasa.gov/allData/tellus/L3/mascon/RL05/JPL/>, supported by the NASA MEASURES Program. The CSR mascons were downloaded at <http://www.csr.utexas.edu/grace>.

### References

- A, G., J. Wahr, and S. Zhong (2013), Computations of the viscoelastic response of a 3-D compressible Earth to surface loading: An application to glacial isostatic adjustment in Antarctica and Canada, *Geophys. J. Int.*, *192*, 557–572, doi:10.1093/gji/ggs030.
- Adhikari, S., and E. R. Ivins, (2016), Climatedriven polar motion: 2003–2015, *Sci. Adv.*, *2*, e1501693, doi:10.1126/sciadv.1501693.
- Alsdorf, D., C. Birkett, T. Dunne, J. Melack, and L. Hess (2001), Water level changes in a large Amazon lake measured with spaceborne radar interferometry and altimetry, *Geophys. Res. Lett.*, *28*, 2671–2674, doi:10.1029/2001GL012962.
- Argo (2000), Argo float data and metadata from Global Data Assembly Centre (Argo GDAC), SEANO, doi:10.17882/42182.
- Bettadpur, S. (2012), UTCSR level-2 processing standards document (revision 4.0) for level-2 product release 0005, GRACE 327-742 The GRACE Project, Center for Space Research, Univ. of Texas at Austin.
- Birkett, C. M. (1995), The contribution of TOPEX/POSEIDON to the global monitoring of climatically sensitive lakes, *J. Geophys. Res.*, *100*(C12), 25,179–25,204, doi:10.1029/95JC02125.
- Cazenave, A., P. Bonnefond, K. Dominh, and P. Shaeffer (1997), Caspian sea level from TopexPoseidon altimetry: Level now falling, *Geophys. Res. Lett.*, *48*, 881–884, doi:10.1029/97GL00809.
- Cazenave, A., and J. L. Chen (2010), Time-variable gravity from space and present-day mass redistribution in the Earth system, *Earth Planet. Sci. Lett.*, *298*, 263–274, doi:10.1016/j.epsl.2010.07.035.
- Chambers, D. P. (2006), Observing seasonal steric sea level variations with GRACE and satellite altimetry, *J. Geophys. Res.*, *111*, C3010, doi:10.1029/2005JC002914.
- Chambers, D. P., J. Wahr, and R. S. Nerem (2004), Preliminary observations of global ocean mass variations with GRACE, *Geophys. Res. Lett.*, *31*, L13310, doi:10.1029/2004GL020461.
- Chen, J. L., C. K. Shum, C. R. Wilson, D. P. Chambers, and B. D. Tapley (2000), Seasonal sea level change from TOPEX/Poseidon observation and thermal contribution, *J. Geod.*, *73*, 638–647.
- Chen, J. L., C. R. Wilson, B. D. Tapley, J. S. Famiglietti, and M. Rodell (2005), Seasonal global mean sea level change from altimeter, GRACE, and geophysical models, *J. Geod.*, *79*(9), 532–539, doi:10.1007/s00190-005-0005-9.
- Chen, J. L., C. R. Wilson, and B. D. Tapley (2006), Satellite gravity measurements confirm accelerated melting of Greenland ice sheet, *Science*, *313*, 1958–1960, doi:10.1126/science.1129007.
- Chen, J. L., C. R. Wilson, B. D. Tapley, D. D. Blankenship, and E. Ivins (2007), Patagonia Icefield melting observed by GRACE, *Geophys. Res. Lett.*, *34*, L22501, doi:10.1029/2007GL031871.
- Chen, J. L., C. R. Wilson, and B. D. Tapley (2011), Interannual variability of Greenland ice losses from satellite gravimetry, *J. Geophys. Res.*, *116*, B07406, doi:10.1029/2010JB007789.
- Chen, J. L., C. R. Wilson, J. C. Ries, and B. D. Tapley (2013), Rapid ice melting drives Earth's pole to the east, *Geophys. Res. Lett.*, *40*, 2625–2630, doi:10.1002/grl.50552.
- Chen, J. L., C. R. Wilson, J. Li, and Z. Zhang (2015), Reducing leakage error in GRACE-observed long-term ice mass change: A case study in West Antarctica, *J. Geod.*, *89*, 925, doi:10.1007/s00190-015-0824-2.
- Chen, J. L., J. S. Famiglietti, B. Scanlon, and M. Rodell (2016), Groundwater storage changes: Present status from GRACE observations, *Surv. Geophys.*, *37*, 397–417, doi:10.1007/s10712-015-9332-4.
- Cheng, M. K., and J. Ries (2015), Monthly estimates of C20 from 5 SLR satellites based on GRACE RL05 models, GRACE Technical Note #07, The GRACE Project, Center for Space Research, Univ. of Texas at Austin. [Available at [ftp://podaac-ftp.jpl.nasa.gov/allData/grace/docs/TN-07\\_C20\\_SLR.txt](ftp://podaac-ftp.jpl.nasa.gov/allData/grace/docs/TN-07_C20_SLR.txt).]
- Cretaux, J.-F., S. Calmant, V. Romanovski, A. Shabunin, F. Lyard, M. Berge-Nguyen, A. Cazenave, F. Hernandez, and F. Perosanz (2009), An absolute calibration site for radar altimeters in the continental domain: Lake Issykkul in Central Asia, *J. Geod.*, *83*(8), 723–735, doi:10.1007/s00190-008-0289-7.
- Cretaux, J.-F., et al. (2011), SOLS: A lake database to monitor in near real time water level and storage variations from remote sensing data, *J. Adv. Space Res.*, *47*(9), 1497–1507, doi:10.1016/j.jasr.2011.01.004.
- Cretaux, J.-F., R. Abarca-Del-Rio, N. M. Bergé, A. Arsen, A. Drolon, G. Clos, and P. Maisongrande (2016), Lake volume monitoring from space, *Surv. Geophys.*, *37*, 269–305, doi:10.1007/s10712-016-9362-6.
- Crossley, D., J. Hinderer, and U. Riccardi (2013), The measurement of surface gravity, *Rep. Prog. Phys.*, *76*, 47, doi:10.1088/0034-4885/76/4/046101.
- Ek, M. B., K. E. Mitchell, Y. Lin, E. Rogers, P. Grunmann, V. Koren, G. Gayno, and J. D. Tarpley (2003), Implementation of the upgraded Noah land-surface model in the NCEP operational mesoscale Eta model, *J. Geophys. Res.*, *108*, 8851, doi:10.1029/2002JD003296.
- Fu, L.-L., and R. A. Davidson (1995), A note on the barotropic response of sea level to time-dependent wind forcing, *J. Geophys. Res.*, *100*, 24,955–24,964, doi:10.1029/95JC02259.
- Gardner, A. S., G. Moholdt, B. Wouters, G. J. Wolken, D. O. Burgess, M. J. Sharp, J. G. Cogley, C. Braun, and C. Labine (2011), Sharply increased mass loss from glaciers and ice caps in the Canadian Arctic Archipelago, *Nature*, *473*(7347), 357–360.
- Humphrey, V., L. Gudmundsson, and S. I. Seneviratne (2016), *Surv. Geophys.*, *37*, 357, doi:10.1007/s10712-016-9367-1.
- Ivins, E. R., M. M. Watkins, D.-N. Yuan, R. Dietrich, G. Casassa, and A. Rülke (2011), On-land ice loss and glacial isostatic adjustment at the Drake Passage: 2003–2009, *J. Geophys. Res.*, *116*, B02403, doi:10.1029/2010JB007607.
- Klige, R. K., and M. S. Myagkov (1992), Changes in the water regime of the Caspian Sea, *GeoJournal*, *27*(3), 299–307.

- Landerer, F. W., and S. C. Swenson (2012), Accuracy of scaled GRACE terrestrial water storage estimates, *Water Resour. Res.*, *48*, W04531, doi:10.1029/2011WR011453.
- Matsuo, K., and K. Heki (2012), Anomalous precipitation signatures of the Arctic Oscillation in the time-variable gravity field by GRACE, *Geophys. J. Int.*, *130*, 1495–1506, doi:10.1111/j.1365-246X.2012.05588.x.
- Ogawa, R., B. F. Chao, and K. Heki (2011), Acceleration signal in GRACE time-variable gravity in relation to interannual hydrological changes, *Geophys. J. Int.*, *184*, 673–679, doi:10.1111/j.1365-246X.2010.04843.x.
- Oleson, K. W., et al. (2010), Technical description of version 4.0 of the Community Land Model (CLM), *NCAR Technical Note NCAR/TN-478+STR*, 257 pp., Natl. Cent. for Atmos. Res., Boulder, Colo.
- Panin, G. (2007), Caspian sea level fluctuations as a consequence of regional climatic change, in *Global Change: Enough Water for All?*, edited by J. L. Lozán et al., pp. 216–219, Wissenschaftliche Auswertungen, Hamburg. [Available at [www.klima-warnsignale.uni-hamburg.de](http://www.klima-warnsignale.uni-hamburg.de).]
- Rodell, M., et al. (2004), The Global Land Data Assimilation System, *Bull. Am. Meteorol. Soc.*, *85*(3), 381–394.
- Rodell, M., I. Velicogna, and J. S. Famiglietti (2009), Satellite-based estimates of groundwater depletion in India, *Nature*, *460*, 999–1002, doi:10.1038/nature08238.
- Roemmich, D., and W. B. Owens (2000), The Argo Project: Global ocean observations for understanding and prediction of climate variability, *Oceanography*, *13*, 45–50.
- Save, H., S. Bettadpur, and B. D. Tapley (2012), Reducing errors in the GRACE gravity solutions using regularization, *J. Geod.*, *86*, 695–711, doi:10.1007/s00190-012-0548-5.
- Save, H., S. Bettadpur, and B. D. Tapley (2016), High resolution CSR GRACE RL05 mascons, *J. Geophys. Res. Solid Earth*, *121*, 7547–7569, doi:10.1002/2016JB013007.
- Scanlon, B. R., Z. Zhang, H. Save, D. N. Wiese, F. W. Landerer, D. Long, L. Longuevergne, and J. L. Chen (2016), Global evaluation of new GRACE mascons products for hydrologic applications, *Water Resour. Res.*, *52*, 9412–9429, doi:10.1002/2016WR019494.
- Schmidt, R., et al. (2006), GRACE observations of changes in continental water storage, *Global Planet. Change*, *50*, 112–126.
- Schrama, E. J. O., B. Wouters, and R. Rietbroek (2014), A mascon approach to assess ice sheet and glacier mass balances and their uncertainties from GRACE data, *J. Geophys. Res. Solid Earth*, *119*, 6048–6066, doi:10.1002/2013JB010923.
- Swenson, S., and J. Wahr (2006), Post-processing removal of correlated errors in GRACE data, *Geophys. Res. Lett.*, *33*, L08402, doi:10.1029/2005GL025285.
- Swenson, S., D. Chambers, and J. Wahr (2008), Estimating geocenter variations from a combination of GRACE and ocean model output, *J. Geophys. Res.*, *113*, B8410, doi:10.1029/2007JB005338.
- Tamisiea, M. E., J. X. Mitrovica, and J. L. Davis (2007), GRACE gravity data constrain ancient ice geometries and continental dynamics over Laurentia, *Science*, *316*, 881–883, doi:10.1126/science.1137157.
- Tapley, B. D., S. Bettadpur, M. M. Watkins, and C. Reigber (2004), The gravity recovery and climate experiment: Mission overview and early results, *Geophys. Res. Lett.*, *31*, L09607, doi:10.1029/2004GL019920.
- Velicogna, I., and J. Wahr (2006), Acceleration of Greenland ice mass loss in Spring 2004, *Nature*, *443*, 329–331, doi:10.1038/nature.05168.
- Wahr, J., M. Molenaar, and F. Bryan (1998), Time-variability of the Earth's gravity field: Hydrological and oceanic effects and their possible detection using GRACE, *J. Geophys. Res.*, *103*(B12), 30,205–30,230, doi:10.1029/98JB02844.
- Wahr, J., S. Swenson, V. Zlotnicki, and I. Velicogna (2004), Time-variable gravity from GRACE: First results, *Geophys. Res. Lett.*, *31*, L11501, doi:10.1029/2004GL019779.
- Watkins, M. M., D. N. Wiese, D.-N. Yuan, C. Boening, and F. W. Landerer (2015), Improved methods for observing Earth's time variable mass distribution with GRACE using spherical cap mascons, *J. Geophys. Res. Solid Earth*, *120*, 2648–2671, doi:10.1002/2014JB011547.
- Wiese, D. N. (2015) GRACE monthly global water mass grids NETCDF RELEASE 5.0. ver. 5.0, PO.DAAC, Calif., doi:10.5067/TEMSC-OCL05.
- Wiese, D. N., F. W. Landerer, and M. M. Watkins (2016), Quantifying and reducing leakage errors in the JPL RL05M GRACE mascon solution, *Water Resour. Res.*, *52*, 7490–7502, doi:10.1002/2016WR019344.
- Wouters, B., D. Chambers, and E. J. O. Schrama (2008), GRACE observes small-scale mass loss in Greenland, *Geophys. Res. Lett.*, *35*, L20501, doi:10.1029/2008GL034816.
- Yi, S., W. Sun, K. Heki, and A. Qian (2015), An increase in the rate of global mean sea level rise since 2010, *Geophys. Res. Lett.*, *42*, 3998–4006, doi:10.1002/2015GL063902.